ONE-STEP SYNTHESIS OF NANOCRYSTALLINE OXIDES WITH UNUSUAL PHYSICAL PROPERTIES. MULLITE-TYPE SOLID SOLUTIONS SYNTHESIZED VIA MECHANOCHEMICAL/THERMAL TREATMENT.

Fabián Martin[1], Santiago T. Rafael[2], Klebso L. Da Silva[2], Kostová Nina[3], Šepelák Vladimír[1]

[1]Institute of Geotechnics, Slovak Academy of Sciences, Kosice, Slovakia, [2] State University of Maringá, Maringá, Brazil, [3]Institute of Catalysis, Bulgarian Academy of Science, Sofia, Bulgaria

fabianm@saske.sk

Abstract: *The one-step synthesis using high energy ball milling can be used in preparation of many complex/doped oxides. In this work we report, as an example, on synthesis and characterization of mullite-type solid solutions. Mullite type $Bi_2(Fe_xGa_{1-x})_4O_9$ solid solutions with $0.1 \leq x \leq 1.0$, were synthesized by combination of mechanochemical and thermal treatments of the Bi_2O_3/α-Fe_2O_3/Ga_2O_3 stoichiometric mixture. The microstructure of the as-prepared materials on the long-range and local atomic scales was investigated by X-ray diffraction and ^{57}Fe Mössbauer spectroscopy, respectively.*

Keywords: Mullite-type solid solution; Bismuth-bearing complex oxide; Rietveld analysis; Mössbauer spectroscopy

1. Introduction

In recent years, the mullite structured bismuth-bearing complex oxides with the general formula of $Bi_2M_4O_9$ (M = Fe^{3+}, Ga^{3+} and Al^{3+}) and their substituted derivatives of the type $Bi_{2-2x}A_{2x}M_4O_{9-x}$ (*e.g.*, A = Sr^{2+}) have become attractive subjects in materials research and applications [1]. It is due to their high thermal stability, good creep resistance, low thermal conductivity, low thermal expansion, anionic conductivity, high emission in the infrared region, etc. [2]. As shown in Figure 1, their structure is characterized by columns of edge-sharing MO_6 octahedrons parallel to the c axis, which are interconnected by double M_2O_7 tetrahedrons. Tetrahedrally coordinated (T) and octahedrally coordinated [O] sites can accept both transition and main group metal cations [3].

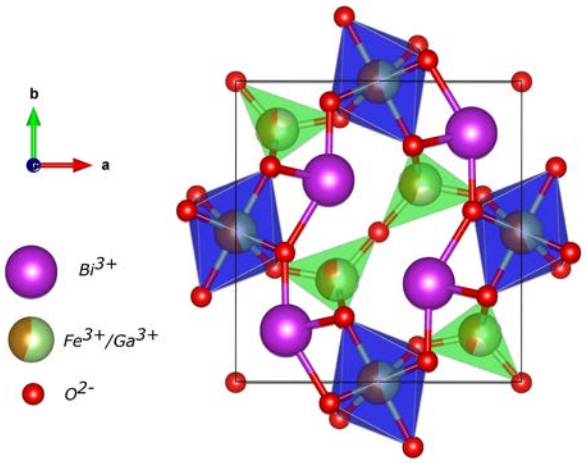

Fig. 1 Crystal structure of mullite-type $Bi_2(Fe_xGa_{1-x})_4O_9$, x = 0.5.

It is well known that functional properties and microstructure of complex oxides are closely related to the processes used for their preparation [4]. In fact, in recent years, several methods have been reported to synthesize bismuth-bearing complex oxides with mullite structure. For example, *Zha et al.* [5] and more recently *Voll et al*. [6] used a glycine-nitrate process to synthesize mullite-type compounds. *Giaquinta et al.* [7] applied a conventional ceramic route to bismuth-bearing oxides, based on the annealing stoichiometric amounts of oxides at 1125 K in air for two weeks with frequent grindings. *Gesing et al.* [8] reported on glycerine- and the EDTA/citric acid synthesis method. In both cases samples were heated at 1023 K for several tens of hours. Pure [9] and doped [10] $Bi_2Al_4O_9$ samples were also prepared by the combustion synthesis route using the glycine-nitrate process and followed by high-temperature annealing at 1323 – 1363 K. In another powder syntheses of $Bi_2Al_4O_9$ and $Bi_2Fe_4O_9$, annealing temperatures in the range from 1123 K to 1273 K were used [11-13].

In this manuscript, the synthesis of mullite-type $Bi_2(Fe_xGa_{1-x})_4O_9$ solid solutions ($0.1 \leq x \leq 1.0$) prepared by mechanochemical treatment of stoichiometric mixtures of the Bi_2O_3/α-Fe_2O_3/Ga_2O_3 precursors, followed by their annealing at the reduced temperature (1073 K), is reported. Although the similar preparation method of mullite-type complex oxides has already been described in our previous work [1,14,15], it should be noted that the precise structural study of the above-mentioned solid solutions has not been performed yet. Based on our previous experience [see *e.g.*, 4,16,17], the simultaneous use of diffraction techniques sensitive to medium- and long-range structural order, and spectroscopic methods, which make possible observations on a local atomic scale, is crucial to reveal structure of the as-synthesized complex oxides properly. In this work, information is provided on the local structure of the as-prepared $Bi_2(Fe_xGa_{1-x})_4O_9$ ($0.1 \leq x \leq 1.0$) solid solutions, including coordinates of the atoms, the unit cell dimensions and the atom occupation factors derived from the Rietveld refinements of X-ray diffraction (XRD) data. Moreover, due to the ability of ^{57}Fe Mössbauer spectroscopy to reveal local environment of Fe nuclei, the effect of iron concentration on the variation in site occupancy, isomer shift and quadrupole splitting in $Bi_2(Fe_xGa_{1-x})_4O_9$ solid solutions is also discussed.

2. Experimental material and method

$Bi_2(Fe_xGa_{1-x})_4O_9$ ($0.1 \leq x \leq 1.0$) solid solutions were prepared from the stoichiometric mixture of Bi_2O_3 (Alfa Aesar, 99.999 %), α-Fe_2O_3 (Alfa Aesar, 99.998 %) and Ga_2O_3 (Alfa Aesar, 99.99 %) powders by the mechanochemical/thermal synthesis using a high-energy planetary ball mill Pulverisette 6 (Fritsch, Germany). The precursors were milled for 3 h at 600 rpm in ambient atmosphere using the chamber (250 cm^3) with 22 balls (10 mm in diameter) both made of tungsten carbide. The ball-to-powder mass ratio was 22:1. After milling, the powdered mixture was calcined at 1073 K in air for 24 h.

XRD patterns were recorded with a PW 1820 X-ray diffractometer (Philips, Netherlands), operating in Bragg configuration, using Cu–Kα radiation (λ = 1.54056 Å). XRD data were collected in the range of 10–80° 2θ with a step size of 0.02° and collection time of 5 s. Rietveld refinements of XRD data of the as-synthesized solid solutions were performed in *Pbam* space group with orthorhombic structure using *Fullprof* software [18]. The XRD line broadening was analyzed by refinement of regular pseudo-Voight function parameters.

^{57}Fe Mössbauer measurements were carried in the transmission mode at room temperature. ^{57}Co in Rh was used as γ-rays source. *Recoil* spectral analysis software was employed for the quantitative analysis of the Mössbauer spectra [19]. The velocity scale and isomer shifts were calibrated using a metallic α-Fe foil absorber at room temperature.

3. Results

The representative XRD patterns of the $Bi_2(Fe_xGa_{1-x})_4O_9$ solid solutions with $0.1 \leq x \leq 1.0$ are shown in Figure 2a. The as-synthesized samples are characterized by narrow diffraction peaks indicating their well-crystallized nature. All diffraction peaks correspond to the orthorhombic mullite-type phase with *Pbam* space group; no spurious or minority phases have been observed. It should be highlighted that in relatively low annealing temperature (1073 K) was applied in the present case. In this context we can conclude that the combined mechanochemical/thermal treatment used in the present study represents an effective, simple, lower-temperature processing route, and thus, a low-cost protocol to synthesize $Bi_2(Fe_xGa_{1-x})_4O_9$ solid solutions.

To gain quantitative information on the structure of the as-synthesized $Bi_2(Fe_xGa_{1-x})_4O_9$ ($0.1 \leq x \leq 1.0$) solid solutions, their XRD data were refined by Rietveld analysis. The representative Rietveld refinement of the XRD data for the $Bi_2(Fe_xGa_{1-x})_4O_9$ sample with x = 0.5 is shown in Figure 2b. Here, the observed data are represented by the open circles and the solid curve represents the result of fitting. The bottom line shows the difference between observed and calculated intensities. The derived crystal structure parameters and the exact atomic positions for the $Bi_2Fe_2Ga_2O_9$ sample are listed in Table 1.

The crystal structure parameters and the goodness parameters of the fits resulting from the Rietveld analyses of the as-prepared solid solutions are listed in Table 2. Rietveld refinements revealed that the cell volume of the as-synthesized samples increases with iron concentration. This effect most likely originates from the replacement of Ga^{3+} by Fe^{3+} ions with different ionic radius (0.49 pm for Fe^{3+} (T) and 0.47 pm for Ga^{3+} (T)) [20]. The lattice parameters of the solid solutions increase linearly with increasing iron content as expected according to the Vergard's law (see Figure 3) [1,7]. In order to reveal the short-range local structure of the as-synthesized solid solutions, in the following we will present and discuss the results obtained by ^{57}Fe Mössbauer spectroscopy. The representative ^{57}Fe Mössbauer spectra of the samples (for x = 0.1, 0.5 and 0.9) are shown in Figure 4. They demonstrate very clearly the presence of two coordination sites for iron cations in the mullite-type structure of $Bi_2(Fe_xGa_{1-x})_4O_9$ solid solutions; *i.e.*, two well-resolved doublets are characteristic for tetrahedrally coordinated (IS = 0.2 mm.s^{-1}, external doublet in Figure 4) and octahedrally coordinated (IS = 0.3 mm.s^{-1}, internal doublet in Figure 4) ferric cations.

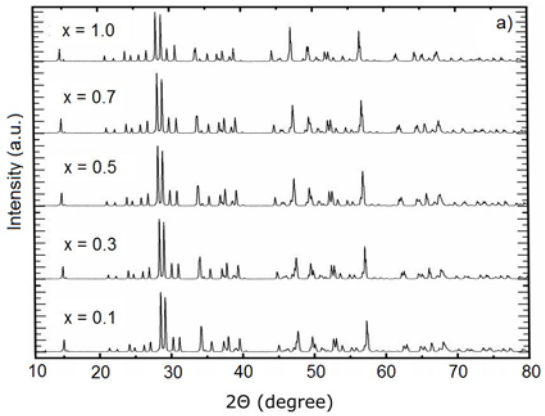

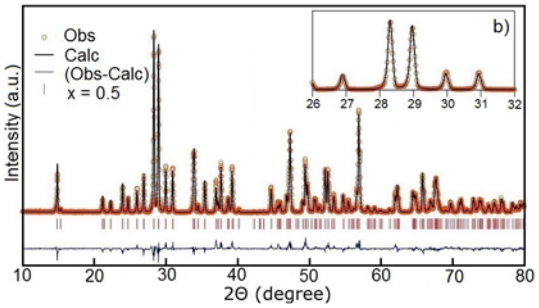

Fig.2. (a) XRD patterns of the as-synthesized $Bi_2(Fe_xGa_{1-x})_4O_9$ solid solutions with $0.1 \leq x \leq 1.0$. (b) Rietveld refinement of the $Bi_2(Fe_xGa_{1-x})_4O_9$ solid solution for x = 0.5.

Table 1
Crystal structure parameters (*a*, *b*, *c* and *V*) and the exact atomic positions (x, y, z) for $Bi_2(Fe_xGa_{1-x})_4O_9$ (x = 0.5) derived from Rietveld refinement of XRD data. R_p, R_{wp} and R_{exp} are the goodness parameters of the refinement.

Empirical Formula: $Bi_2Fe_2Ga_2O_9$
Crystal System: orthorhombic
Space Group: *Pbam* (No. 55)
***a* (Å) =** 7.9552(3)
***b* (Å) =** 8.3746(3)
***c* (Å) =** 5.9503(2)
***V* (Å³) =** 396.424(2)

Atomic position	**x**	**y**	**z**
Fe_1 – 4f	0.50000	0.00000	0.2609(7)
Fe_2 – 4h	0.3547(4)	0.3411(5)	0.50000
Ga_1 – 4f	0.50000	0.00000	0.2609(7)
Ga_2 – 4h	0.3547(4)	0.3411(5)	0.50000
O_1 – 2b	0.00000	0.00000	0.50000
O_2 – 8i	0.3794(9)	0.2147(13)	0.2474(18)
O_3 – 4h	0.1365(12)	0.380(3)	0.50000
O_4 – 4g	0.1708(18)	0.4303(12)	0.50000
R-values (%)	R_p = 11.4	R_{wp} = 14.3	R_{exp} = 7.88
Fe_1 – 4f	0.50000	0.00000	0.2609(7)

They demonstrate very clearly the presence of two coordination sites for iron cations in the mullite-type structure of $Bi_2(Fe_xGa_{1-x})_4O_9$ solid solutions; *i.e.*, two well-resolved doublets are characteristic for tetrahedrally coordinated (IS = 0.2 mm.s^{-1}, external doublet in Figure 4) and octahedrally coordinated (IS = 0.3 mm.s^{-1}, internal doublet in Figure 4) ferric cations.

Table 2
Lattice parameters (*a*, *b* and *c*), for $Bi_2(Fe_xGa_{1-x})_4O_9$ solid solutions.

x	***a* (Å)**	***b* (Å)**	***c* (Å)**
0.1	7.930	8.323	5.908
0.2	7.940	8.335	5.919
0.3	7.949	8.348	5.930
0.5	7.955	8.375	5.950
0.7	7.967	8.406	5.975
0.8	7.964	8.416	5.983
0.9	7.969	8.432	5.995

Fig. 3. Lattice parameters (*a*, *b*, *c*) and lattice volume (*V*) of the $Bi_2(Fe_xGa_{1-x})_4O_9$ solid solutions as a function of iron content (x).

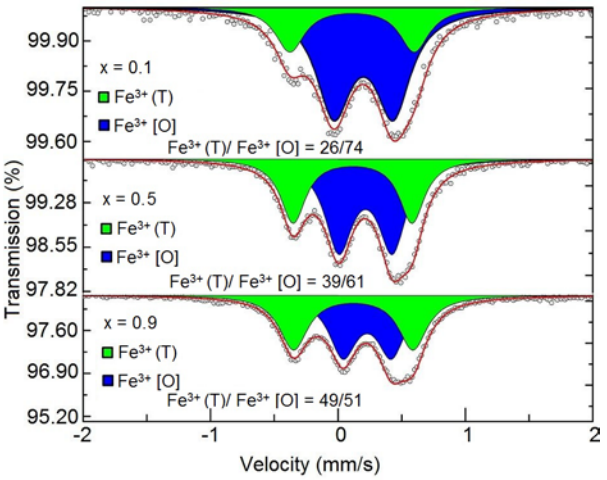

Fig. 4. ^{57}Fe Mössbauer spectra of selected $Bi_2(Fe_xGa_{1-x})_4O_9$ solid solutions (for x = 0.1, 0.5 and 0.9) measured at room temperature. The open circles represent measured data and solid lines (red) represents the fitting curves. The subspectra corresponding to tetrahedrally and octahedrally coordinated ferric cations are denoted as Fe^{3+}(T) and Fe^{3+}[O], respectively. Subspectral area fractions Fe^{3+}(T)/Fe^{3+}[O] are also indicated.

4. Conclusion

Mullite-type $Bi_2(Fe_xGa_{1-x})_4O_9$ solid solutions with $0.1 \leq x \leq 1.0$ were synthesized by high-energy ball milling of Bi_2O_3/α-Fe_2O_3/Ga_2O_3 stoichiometric mixtures followed by subsequent annealing at 1073 K for 24 h. Relatively short time and lower temperature of the combined mechanochemical/thermal synthesis of the $Bi_2(Fe_xGa_{1-x})_4O_9$ mixed crystals is ascribed to the pre-activation of the reaction precursors. The long-range and short-range structures of the as-prepared samples were characterized by XRD and ^{57}Fe Mössbauer spectroscopy. Rietveld refinements of the mixed crystals revealed that their lattice parameters vary linearly with iron content and change in accordance with Vegard's law. ^{57}Fe Mössbauer spectra of all investigated samples distinguished tetrahedrally and octahedrally coordinated Fe^{3+} cations.

Acknowledgments

This work was supported by the Visegrad Group (V4) – Japan Joint Research Program on Advanced Materials *"Structure-Function Relationship of Advanced Nanooxides for Energy Storage Devices (AdOX)"*, the VEGA (projects 2/0128/16 and 2/0097/14) and by the APVV (project SK-BG 2013-0011). M.F. thanks FA/CAPES agency (project 12/2013-FA).

References

1 K. L. Da Silva, V. Šepelák, A. Paesano Jr, F. J. Litterst, K.-D. Becker, Z. Anorg. Allg. Chem., 636 (2010) 1018.
2 S. Komarneni, H. Schneider and K. Okada, (2005) Mullite Synthesis and Processing, in Mullite (eds H. Schneider and S. Komarneni), Wiley-VCH Verlag GmbH & Co. KGaA, Weinheim, FRG.
3 M. Liu, H. Yang, Y. Lin, Y. Yang, J. Mater. Sci.: Mater. Electron., 25 (2014) 4949.
4 M. Fabián, P. Bottke, V. Girman, A. Düvel, K. L. Da Silva, M. Wilkening, H. Hahn, P. Heitjans, V. Šepelák, RSC Advances, 5 (2015) 54321.
5 S. Zha, J. Cheng, Y. Liu, X. Liu, G. Meng, Solid State Ionics, 156 (2003) 197.
6 D. Voll, A. Beran, H. Schneider, Phys. Chem. Minerals, 33 (2006) 623.
7 D. M. Giaquinta, G. C. Papaefthymiou, W.M. Davis, H.-C. zur Loye, J. Solid State Chem., 99 (1992) 120.
8 Gesing, T.M., Fischer, R.X., Burianek, M., Mühlberg, M., Debnath, T., Rüscher, C.H., Ottinger, J., Buhl, J.-Ch., Schneider, H., J. Eur. Ceram. Soc., 31 (2011) 3055.
9 I. Bloom, M. C. Hash, J. P. Zebrowski, K. Myles, M. Krumpelt, Solid State Ionics, 53-56 (1992) 739.
10 S. Zha Cheng, Y. Liu, X. Liu, G. Meng, Solid State Ionics, 156 (2003) 197.
11 R. Arpe, H. K. Muller-Buschbaum, J. Inorg. Nucl. Chem., 39 (1977) 233.
12 I. Abrahams, A. J. Bush, G. E. Hawkes, T. Nunes, J. Solid State Chem., 147 (1999) 631.
13 A. S. Poghossian, H. V. Abovian, P. B. Avakian, S. H. Mkrtchian, V. M. Haroutunian, Sensors Actuators B, 4 (1991) 545.
14 K. L. Da Silva, V. Šepelák, A. Düvel, A. Paesano Jr., H. Hahn, F. J. Litterst, P. Heitjans, K. D. Becker. J. Solid State Chem., 184 (2011) 1346.
15 K. L. Da Silva, C. F. C. Machado, M. Fabián, M. Harničárová, J. Valíček, H. Hahn, V. Šepelák, Mater. Lett., 161 (2015) 488.
16 V. Šepelák, M. Myndyk, M. Fabián, K. L. Da Silva, A. Feldhoff, D. Menzel, M. Ghafari, H. Hahn, P. Heitjans, K. D. Becker, Chem. Commun., 48 (2012) 11121.
17 M. Fabián, B. Antić, V. Girman, M. Vučinić-Vasić, A. Kremenović, S. Suzuki, H. Hahn, V. Šepelák, J. Solid State Chem., 230 (2015) 42.
18 J. Rodriguez-Carvajal, Fullprof, version 3.0.0, ILL Grenoble, Grenoble, France, 2015.
19 K. Lagarec, D. G. Rancourt, Recoil-Mössbauer Spectral Analysis Software for Windows, Version1.02; Department of Physics, University of Ottawa, Ottawa, Canada, 1998.
20 R. D. Shannon, Acta Crystallogr. A, 32 (1976) 751.